Original Article
CNJ.araku.ac.ir
Cite This: Colloid & Nanoscience Journal 2(2) (2024) 304-320.

# Surface modification of polyethersulfone nanofiltration membranes by nanocomposite Layer containing POSS nanoparticles

**Abdolreza Moghadassi[1*], Maryam Ghaffari[1], Samaneh Bandehali[2*], Narjes Rabiei Karahroudi[1]**

**Received:**2024-10-29
**Revised:** 2024-11-01
**Accepted:** 2024-11-01
DOI: **10.61186/CNJ.2.2.304**

[1]Department of Chemical Engineering, Arak University, Arak 38156-8-8349, Iran

[2]Department of Mechanical Engineering, Ayatollah Boroujerdi University, Boroujerd 69199-69737, Iran

**Abstract**

In this research, a nanocomposite layer containing POSS nanoparticles was applied to improve the properties and surface modification of polyether sulfone nanofiltration membranes. The impact of the Surface modification, on the structure, separation, and other properties of the membranes was checked. The pristine membranes were prepared via the phase inversion method. Also, the surface of the membrane was modified by the dip coating method. The characterization of the fabricated membranes was done by FTIR, SEM and AFM analysis. Moreover, the separation performance of membranes was examined by the contact angle, porosity measurement, water content, pure water flux (PWF), $Na_2SO_4$ rejection, $CrSO_4$ rejection and flux recovery ratio (FRR%). The FTIR results proved the creation of a nanocomposite layer with the POSS nanoparticles on the surface of the virginal membrane. SEM images demonstrated the presence of a new layer on the surface of the modified membranes, exhibiting uniform distribution. The amount of water content for double-layer membranes exhibited an increasing trend in comparison to virginal membranes. Also, the results of the contact angle showed a decrease in the surface roughness for the modified membranes then with increasing concentration of glycidyl-pass nanoparticles, that is a hydrophobic substance, went through a decreasing trend. By increasing Acrylic Acid, the porosity was enhanced but after utilizing glycidyl-pass nanoparticles, it showed a decreasing trend. Also, the pure water flux showed a decreasing trend. The rate of return had an increasing trend for the membranes. The addition of glycidyl-pass nanoparticles up to 0.1% by weight resulted in the yield of 59.74% $Na_2SO_4$ and 64% for $CrSO_4$.

**Keywords:** Nanofiltration membrane, Surface modification, Acrylic acid, Glycidyl poss

## 1. Introduction

During the last years, the deficiency of fresh water resources also the increment of requests for clean water have been the major challenges in the world. Moreover, with the growth of pollutants and the presence of high amounts of sulfate, bacteria, chloride, etc. in underground water sources, the application of new technologies with lower energy and cost for purification wastewater treatment and returning water to the life cycle, increased [1-5]. Membrane technology, adsorption, ion exchange, flotation, evaporation, etc. are examples of low-cost and practical methods in the field of water purification. Among these, membrane technology with high separation efficiency, energy saving, combining with other separation processes (hybrid processing), easy to up-scaling, etc. has been noticed [6-8,5]. Nanofiltration membranes are a specific type of pressure-driven membrane. Water purification, desalination, and the ability to take away heavy metals from water are among the applications of nanofiltration during the recent years [9-14]. In addition to the benefits that polymer membranes have, such as simple manufacturing, energy saving, and easy industrialization, they have some defects, including unstable flux, poor antifouling property, and concentration polarization that recently, their modification is a way to reduce their defects. There are various ways such as utilizing





Corresponding Authors: Alireza Khademi
alikhademi54@ut.ac.ir

various polymers and nanoparticles, plasma modification, and chemical modification methods such as free-radical grafting that can be used as a solution to overcome these defects [9,11-15]. Polyethersulfone is a type of polymer material that has been employed to prepare nanofiltration membranes because of high mechanical and thermal stability but PES is a hydrophobic polymer that makes low permeability for the membranes with on increasing trend of fouling [14-18].

In this research, the surface of polyether sulfone nanofiltration membranes was modified through a nanocomposite layer containing POSS nanoparticles for use in the water recovery process. PAS is a nanoparticle that contains Si atoms, and this nanoparticle consists of a cage-like nucleus and functional groups. PAS as a three-dimensional nanoparticle is unique and has been researched for the last 50 years. The chemical formula of PAS is $(C_6H_{11}O_2)_m(SiO_{1.5})_n$, where -R are groups that can be connected at the top and around the PAS, such as halogens, alkenes, alkyls, and hydrogen. Among the advantages of this nanoparticles, we can mention its non-flammability, thermal stability, and high permeability [18]. According to the above advantages, PAS is a hydrophobic nanoparticle, this property causes the limited use of this type of membranes in wastewater treatment [19,20-22]. Nanoparticles of acrylic acid have been used to improve the hydrophobicity of Glycidal-Pas. Acrylic acid is a member of the carboxylic acid group. Also, it contains a vinyl group that attached to another group that named carboxylic acid. Acrylic acid has hydrophilicity, sensitivity to pH, reactivity, and low absorption [23,24]. It is expected that utilizing of nanocomposite layer containing PAS next to acrylic acid nanoparticles will improve the properties of the membrane.

## 2. Material and method

### 2.1 Materials

Polyether sulfone (Mw=5800 g/mol), was used as a virgin membrane-forming polymer. Polyvinylpyrrolidone (Mw=25000 g/mol) as pore forming was prepared from Merck, Germany. Dimethylacetamide was purchased from Swiss Fluka for utilizing as a solvent, and Glycidyl-poss as a surface modifier was purchased from the Polymer and Petrochemical Research Institute. Also, Acrylic acid, potassium persulfate, ethylene glycol was obtained from Merck, Germany. In addition, ($Na_2SO_4$) solution with Mw = 142.04 g/mol, and ($CrSO_4$) with Mw = 156.056 g/mol were applied for the tests.

### 2.2. Preparation and surface modification of nanofiltration membrane

The phase inversion method was employed to produce virginal membranes. A constant concentration of 1% by weight of polyvinylpyrrolidone and 18% by weight of Dimethylacetamide solvent was used to make the membranes. A magnetic stirrer was applied for a period of five hours to facilitate the complete dissolution of the polymer in the solvent, and Air bubbles completely remove from prepared uniform solution by leaving at room for half day. After that, the obtained solution was casted on the glass by an applicator with a thickness of 150 µm, and at once immersed into a DI water bath until the phase change occurred. Finally, the neat membranes were formed by exchange between solvent and non-solvent. Following the preparation of the membranes, they were subjected to a 24-hour deionized water bath to facilitate the complete removal of the solvent. Subsequently, the membranes were placed between two sieves for 24 hours to facilitate the drying process. Then, the surface modifications were done by using the dip-coating method. Surface modifying solutions with different gels of Glycidyl-Pass by dissolving 0.05 mg of potassium persulfate in 2 mg of ethylene glycol, 0.08 mg of acrylic acid, and 30 mg of distilled water was made. The prepared solutions were stirred for 15 minutes by a magnetic stirrer. After the complete uniformity of the solutions, various amounts of glycidyl poss were added to them. For better distribution of nanoparticles in the prepared solutions, an ultrasonic bath was used for 15 minutes. Then, to carry out the chemical reaction between acrylic acid and glycidyl poss (AA-g-POSS), the solutions are placed on a magnetic stirrer at a temperature of 50 degrees Celsius for 4 hours. The polyethersulfone nanofilter membranes were immersed in the surface modifying solutions. After removing the membrane from the surface modifying solutions, the polymerization process on the surface of the membranes was completed by placing them in an oven with a temperature of 60 $^{o}$C for 3 hours. The fabricated membranes were named $M_1$ (neat membrane), $M_2$, $M_3$, and $M_4$, respectively. The characteristics of the evaluated membranes are presented in Table 1.

**Table 1.** Introducing virgin and surface-modified membranes.

| Membrane | PES (wt.%) | PVP wt.%) | Acrylic acid (wt.%) | glycidyl POSS (wt.%) |
|---|---|---|---|---|
| $M_1$ | 18 | 1 | 0 | 0 |
| $M_2$ | 18 | 1 | 0.25 | 0 |
| $M_3$ | 18 | 1 | 0.249 | 0.03 |
| $M_4$ | 18 | 1 | 0.248 | 0.3 |

## 2.3. Membrane characterizations

### 2.3.1. Identification analyses

The FTIR analysis, The SEM analysis, The X-ray energy analyzer, and the Atomic AFM were applied to earn information about the membrane characterization.

### 2.3.2. Water content and water contact angle

To assess surface hydrophilicity, the amount of roughness, and wettability, water contact angle and water content were employed. For reducing the error of the test, all experiments were applied about three times for each sample and, the final value was an average of the obtained numbers. It should be noted that, the operational condition was environmental conditions. From Eq. (1) to calculate the water content of the membranes was used [9-11,25,26]:

$$Water\ content = \frac{W_w - W_d}{W_d} \times 100 \quad (1)$$

That, the weight of the wet membranes ($W_w$) is measured by placing the membranes in deionized water for three days. The weight of the dry membranes ($W_d$) is measured by placing the membranes in an oven set to 60°C for one day.

### 2.3.3. The porosity of the membrane

From Eq. (2) to calculate the overall porosity (ε) of fabricated membranes was used [27]:

$$\varepsilon(\%) = \frac{W_w - W_d}{\rho_f V_m} \times 100 \quad (2)$$

Where, the weight of wet membranes(g) is shown by $W_w$, the weight of dry membranes (g) is shown by $W_d$, and the water density ($g/m^3$) is shown by $\rho_f$.

### 2.3.4 The mean pores size of membrane

To calculate the average radius of the pores, the Guerout-Elford-Ferry equation is used, which follows this formula [28]:

$$r_m = \sqrt{\frac{(2.9 - 1.75\varepsilon)8\eta LQ}{\varepsilon A \Delta p}} \quad (3)$$

Where, η is the water viscosity ($8.9 \times 10^{-4}$ Pa.s), L is thickness of membrane (m), Q is the pure water flux (m3/s), and ΔP is operating pressure [28].

### 2.3.5 The flux and salt rejection

The schematic of the nanofiltration system is presented in Fig.1. Nitrogen gas was employed as the driving force for mass transfer and actually supplying the pressure of the used tank. And, during the experiment, the feed was continuously agitated to decrease the results of concentration polarization [29-31].

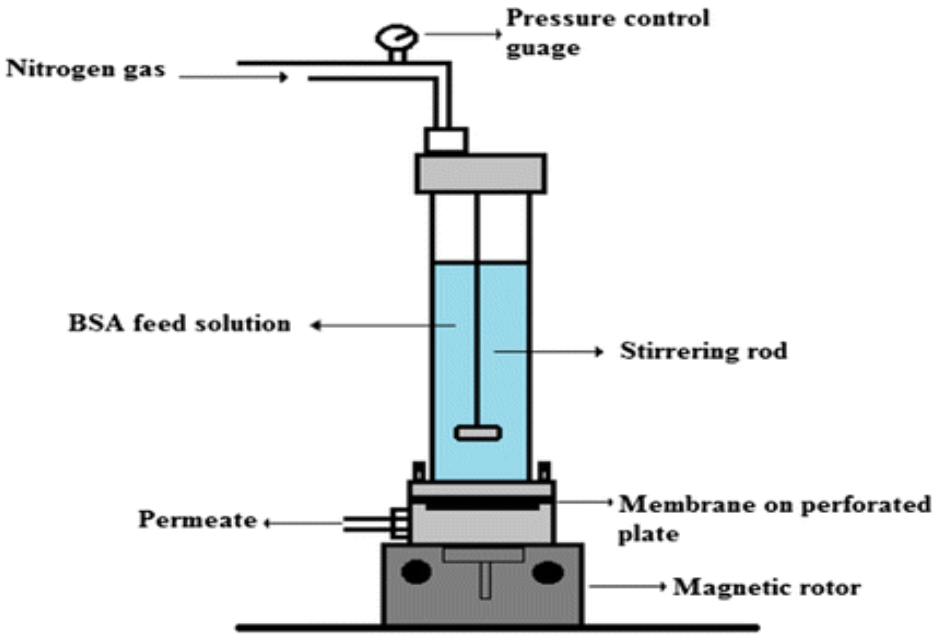


**Fig.1.** The schematic of nanofiltration system [29-31].

The following equation is used to measure the flux [29]:

$$J_{w,1} = \frac{V}{A \times T} \quad (4)$$

Where, the flux (L/m$^2$.h) is shown by J, the membrane surface area (m$^2$) is shown by A, the volume of collected permeation (L) is shown by V, and T is the filtration time (h) [9,10].
Also, the Eq.5 gives us a relationship to calculate the amount of membrane excretion [26]:

$$R(\%) = \left(1 - \frac{C_p}{C_f}\right) \times 100 \quad (5)$$

Where, $C_p$ and $C_f$ are salt concentrations in permeate and feed solutions, respectively [29].

### 2.3.6 flux recovery ratio (FRR%)

From Eq. (6) to calculate the flux recovery (FRR%) was used was measured [28,29]:
That, the pure water flux after washing of fouled membranes by deionized water is shown by $J_{w,2}$.

$$FRR(\%) = \left(\frac{J_{w,2}}{J_{w,1}}\right) \times 100 \quad (6)$$

### 2.3.7. The membrane's mechanical tensile strength

Tensile strength can be defined as the maximum strain that a material can withstand when stretched before tearing or breaking. ASTM1922-03 standard can use to measure this test. Two mechanical clamps and a number of weights with different weights were used to measure the resistance change of the prepared membranes. First, the membranes are cut to the standard size, and in the next step, a mechanical clamp is connected to another clamp, which has the ability to add weight. The weights are placed one by one so that the membrane breaks due to tension. With this method, the tensile strength of the membrane is obtained [9-11].

## 3. Results and discussion

### 3.1. FTIR test results

FTIR analysis was applied to obtain information about functional groups, identify compounds and bonds present in the membrane structure. FTIR result of virgin and modified membrane shows in Fig.2. The peak around the 1073/17 $cm^{-1}$ and 1106/17 $cm^{-1}$, It is a confirmation of the presence of the Si-O-Si function group on the modified membrane surface. Also, the peak around the 2956.28 $cm^{-1}$ confirmed the existence of the glycidyl function group on the modified membrane surface [30-34]. As a result, the change of vibrations at the wavelength of 16.3069 $cm^{-1}$ and 13097 $cm^{-1}$ is also due to the hydroxyl (OH) functional group. The peak at 1667.139 $cm^{-1}$ is ascribed to the (C=O) function group, the peak in the range of 1242-1296 $cm^{-1}$ belongs to ($C=SO_2=C$) function group, and the peak around the 1579-1486 $cm^{-1}$ confirming the presence of a benzene ring in the PES structure [9-11,34].

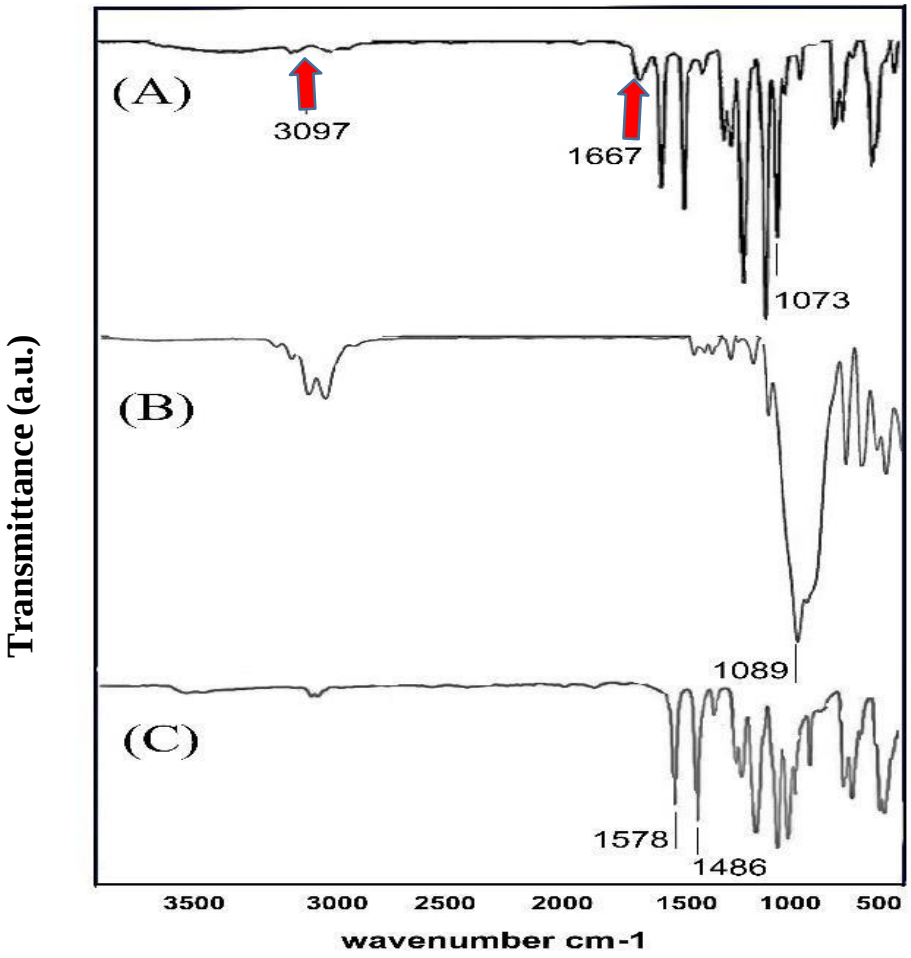


**Fig.2.** FTIR analysis of modified membrane M4 (A), glycidyl-pass (B) and pure polyethersulfone (C).

### 3.2. SEM and EDX results

SEM analysis was utilized to gain insight into the asymmetric structure of the membranes. SEM images of neat and modified membrane shows in Fig.3 The SEM images corroborated the hypothesis that the asymmetric membranes were composed of two distinct layers. The upper layer and the lower layer, which have a spongy-like and finger-like structure, respectively. As illustrated in the accompanying figure, the surface modification of the membrane resulted in a notable increase in the thickness of the dense layer on the membrane surface. This increase indicates the formation of a thin layer on the surface of the primary membrane after modification, which causes a decrease in flux. In comparison to the modified membrane, the surface of the pristine membrane is much smoother. Additionally, the presence of glycidyl Poss nanoparticles increased the surface roughness, resulting in a decrease in hydrophobicity and an increase in clogging, which eventually led to a reduction in pore size (Fig. 4) [36-39].

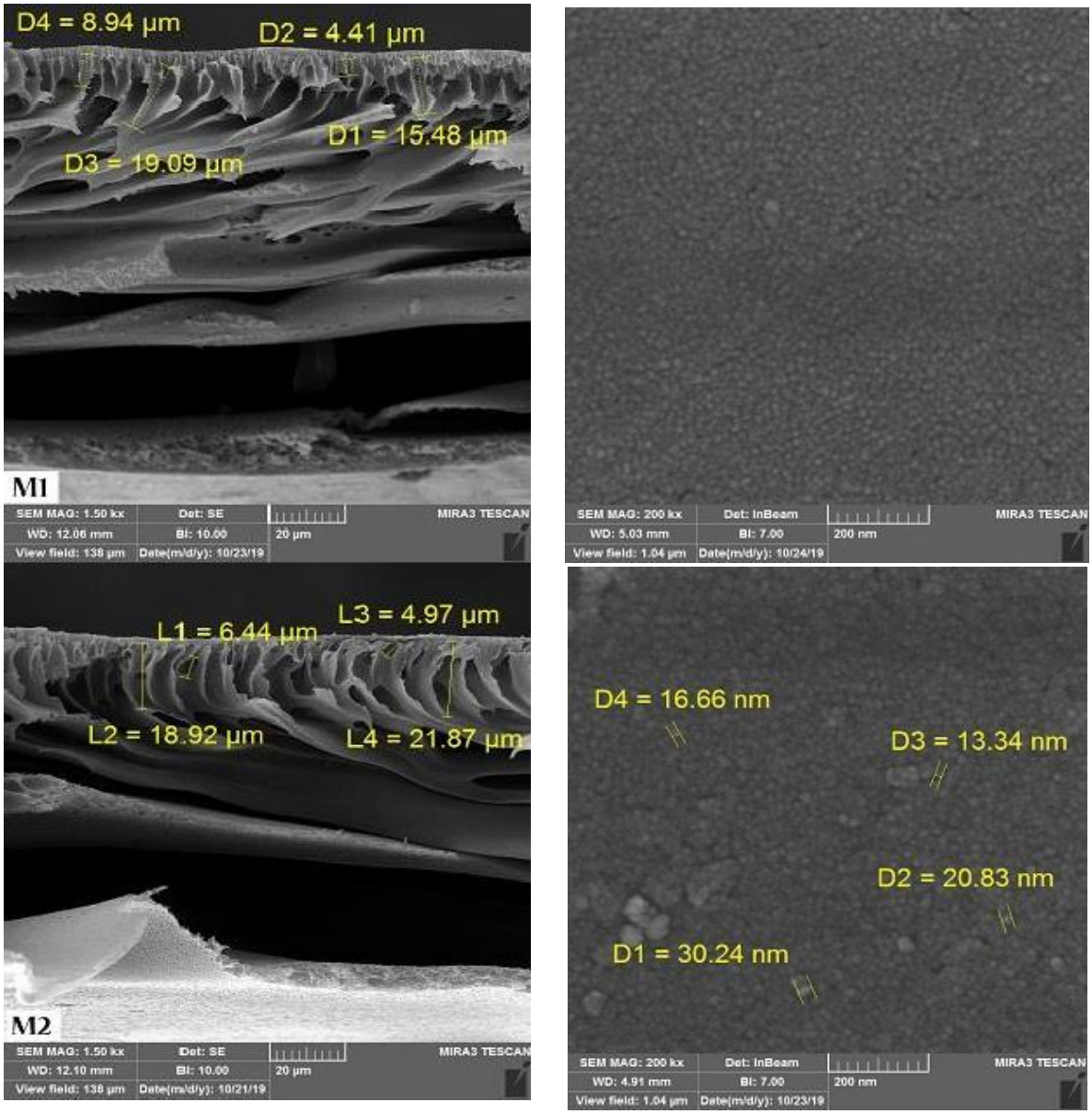

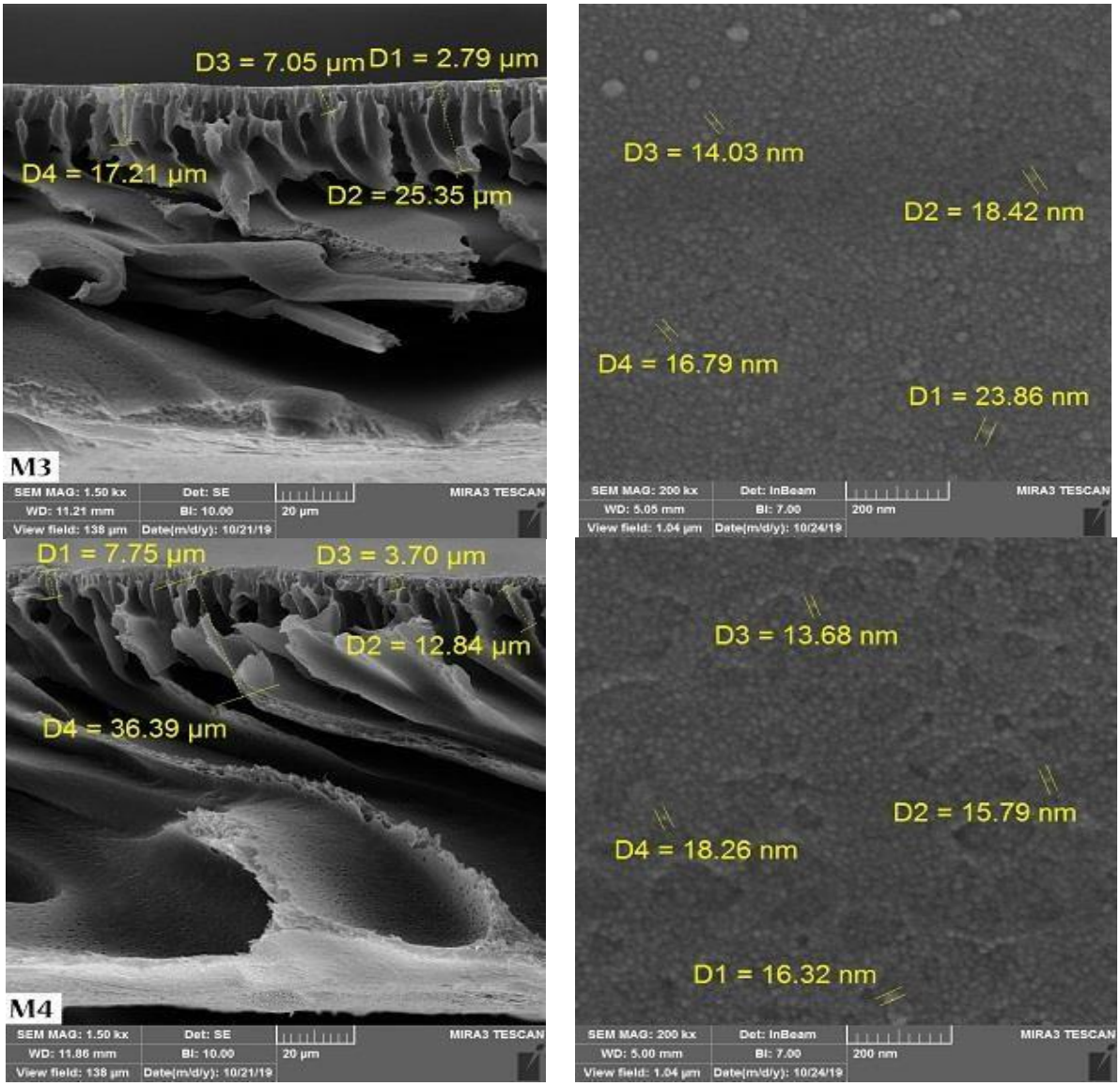


**Fig. 3.** The SEM image; (M1) neat membrane, (M2 to M3) modified membrane

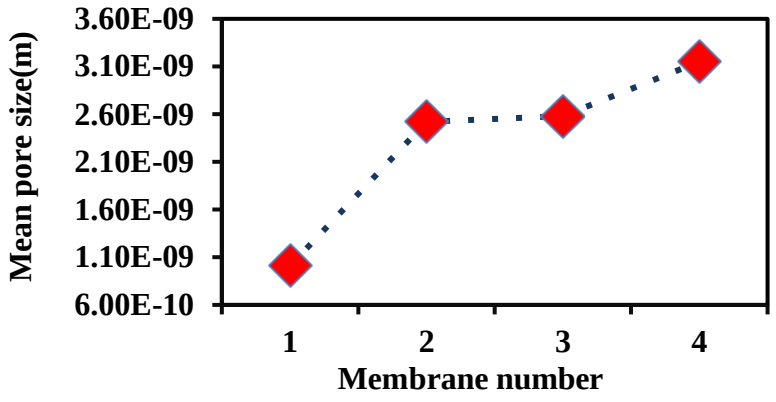


**Fig.4.** The result of the mean pore size

The formation of a uniform layer of Si on the surface of the modified membranes was confirmed by EDX mapping. The EDX results is shown in (Fig.5). Also, the peak of the graph related to Si in the surface of the modified membrane.

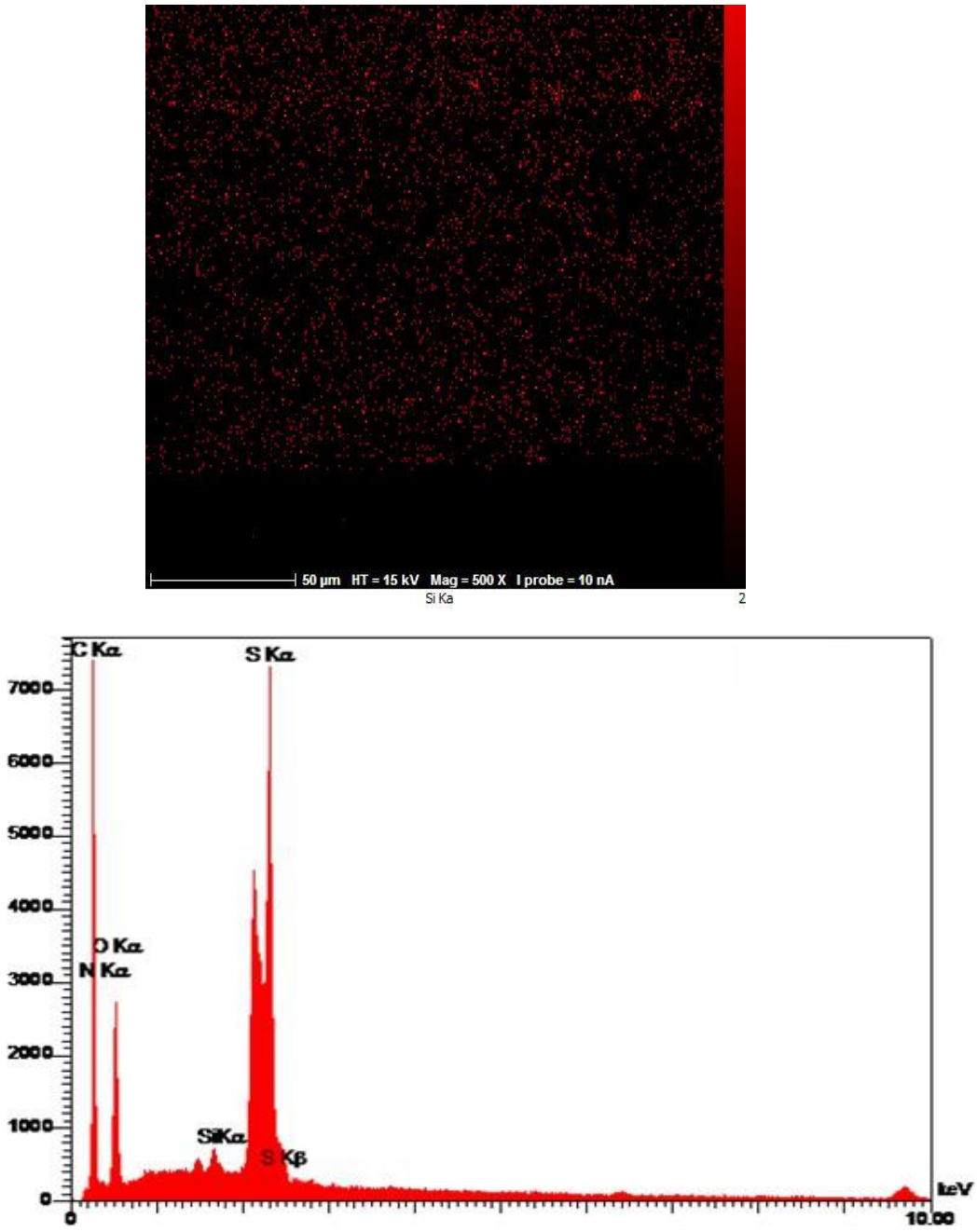


**Fig.5.** The EDX mapping analysis of modified membrane.

The 3D surface images were applied to check the trend of the roughness. The results of 3D surface images are shown in (Fig. 6), Also the calculated average roughness (Ra) is reported (Table.2) [39]. According to the results, by utilizing

glycidyl-pass nanoparticles in the surface of the modified membranes, the trend of the roughness was enhanced, also flux had a decreasing trend and the trend of the clogging had an increasing trend [36-39].

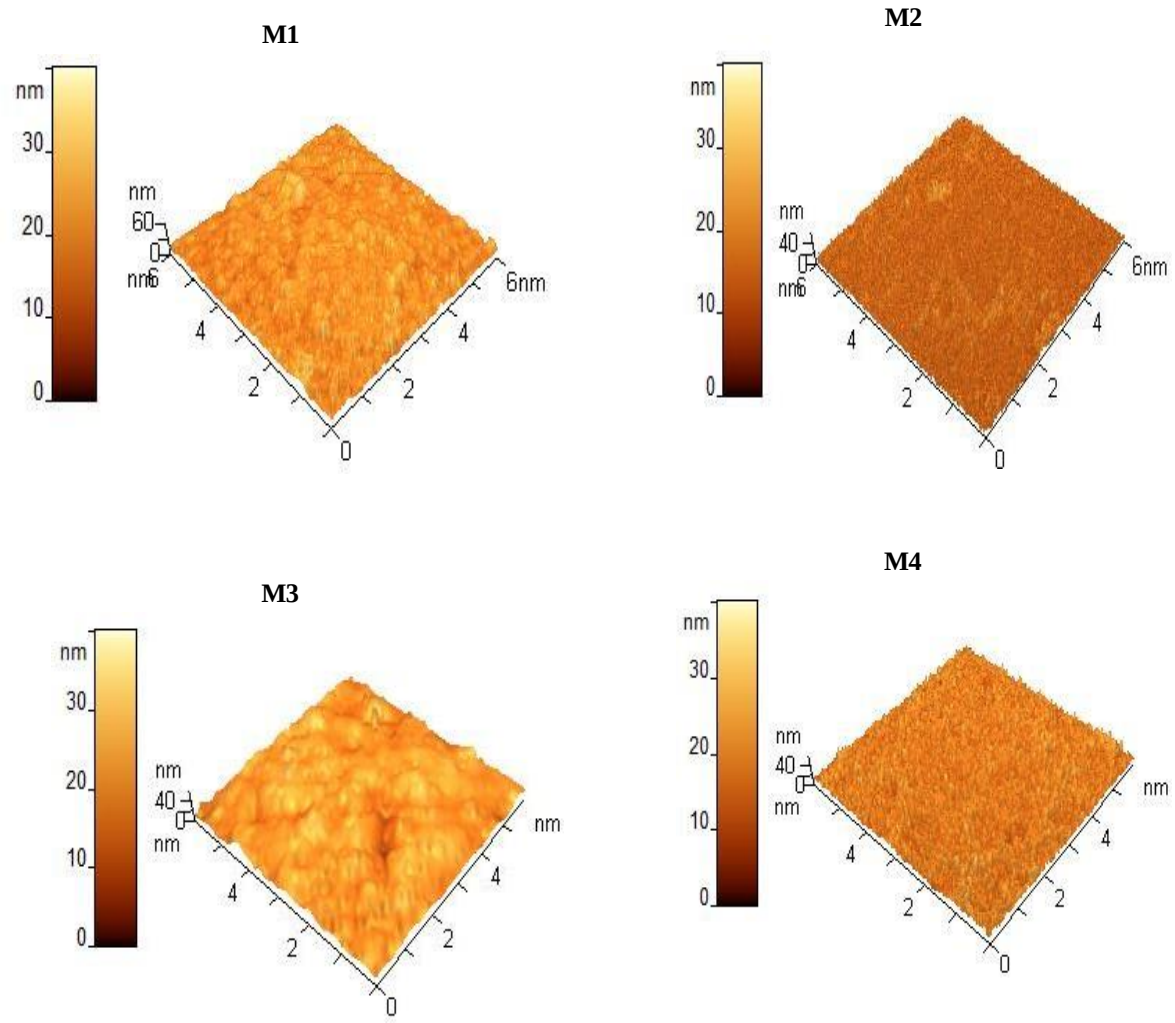


**Fig.6.** 3D surface images of neat and modified membrane.

**Table.2.** The results of the roughness.

| Membrane number | Ra(nm) | Rq(nm) |
|---|---|---|
| M1 | 3.084 | **3.976** |
| M2 | 2.507 | **3.198** |
| M3 | 4.206 | **5.258** |
| M4 | 3.328 | **4.194** |

### 3.3. Water content and water contact angle

Contact angle analysis and water content were employed to investigate the hydrophilicity/ Surface roughness rate and the surface wettability for Fabricated membranes compared to the neat membrane [40]. The results of the contact angle and water content show in Fig.7 and Fig.8 respectively. The findings indicate that the contact angle and Surface roughness rate for the $M_2$ membrane surface were decreased. Also, the hydrophilicity and water content of the $M_2$ membrane surface were enhanced, which can be attributed to the hydrophilic properties of acrylic acid on the M2 membrane surface, including a negative charge caused by the functional groups [11,39,40]. The amount of hydrophilicity in $M_3$ and $M_4$ membranes decreased with the formation of AA-g-POSS on the membrane surface, which could be the result of the accumulation of nanoparticles in pores of the membrane, which caused the reduction of the active surface area of the membrane. Also, water content of the $M_3$ membrane surface were enhanced because by increasing the rate of the hydrophilicity, the surface tendency of the membrane to absorb and retain water in its structure increases but water content of the $M_4$membrane surface were decreased that Part of this change can be due to the hydrophobic property of glycidyl-pass, and another part is due to the filling of surface pores of the membrane with nanoparticles, which reduces the capacity of the membrane to retain and absorb water on the surface and inside the pores of the membrane [40-44].

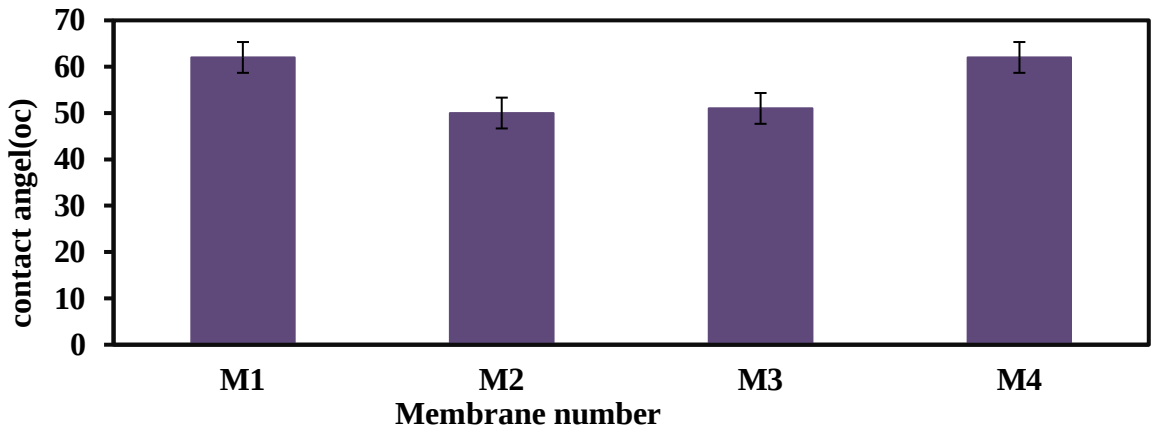


**Fig.7.** The result of the contact angle

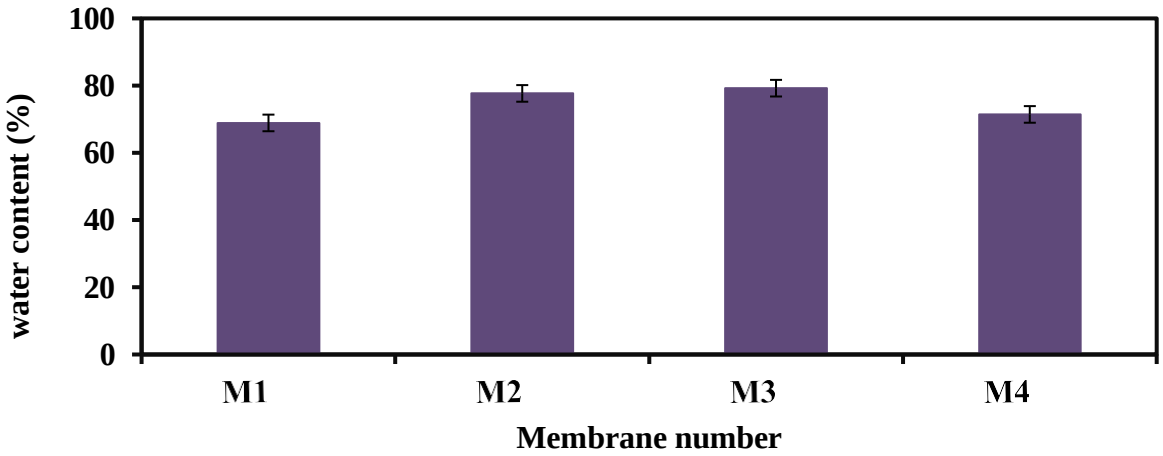


**Fig.7.** The result of the water content (%)

### 3.4. Pure water flux

The results of pure water flux are shown in Fig. 9. According to the result, the pure water flux has decreased at first, then had an increasing trend and decreased again. Also, the water flux of all the modified membranes is lower than the pristine membrane, which can be attributed to the dense layer on the surface of the modified membranes. The decreasing trend of flux for the $M_2$ membrane compared to the primary polyethersulfone membrane is observed because of the dense layer created by the polymerization of acrylic acid on the surface of the membrane. Also, the process of flux increase in $M_3$ membrane with the presence of AA-g-POSS on the surface of the membrane is due to the cage-like structure of Glycidyl-POS, which increases the water passage. In the M4 membrane, the flux of pure water had a decreasing trend, and the increase in the concentration and accumulation of glycidyl-pass nanoparticles causes the clogging of some surface cavities due to the blocking of the transfer channels and the reduction of the flux [9-12,43-45].

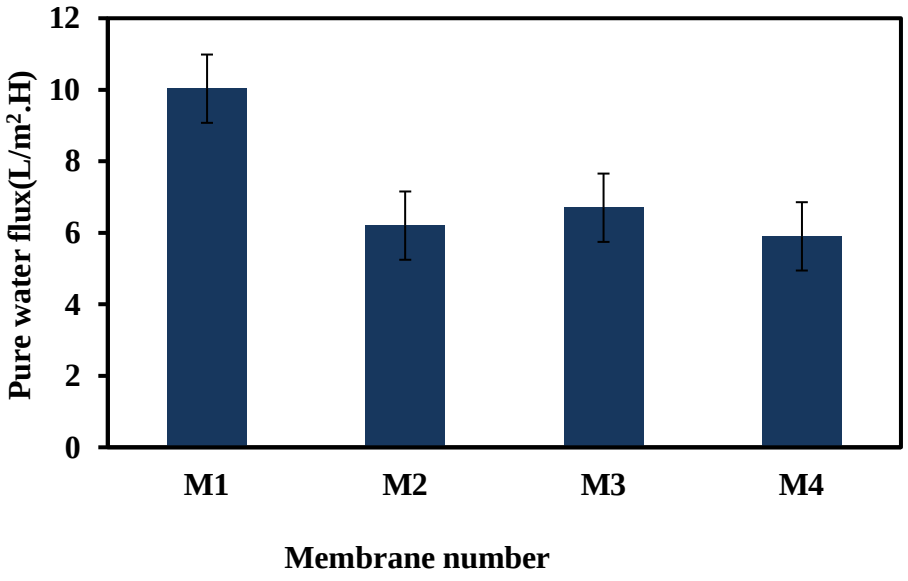


**Fig.9.** Pure water flux

### 3.5. Salt rejection and flux

The result of the $Na_2SO_4$ rejection shows in Fig.10. As a result, the recovery rate of sodium sulfate in the modified membranes was higher than neat membrane. The presence of negatively charged hydroxyl and carboxyl groups in the acrylic acid structure enables the removal of $SO_4^{2-}$ ions. The electrostatic repulsion resulting from the negative charge of the membrane surface and sulfate ions is a significant factor influencing the separation process [46,47]. Consequently, the polymerization of acrylic acid on the surface of the M2 membrane results in an increase in the amount of electrostatic repulsion of SO4-2 ions [46,48]. In $M_3$ and M4 membranes, glycidyl-pass along with acrylic acid is polymerized on the surface of the membrane. The porous and octahedral structure of glycidyl pas causes the creation of active sites and the inclusion of more functional groups around the glycidyl pas, and this causes the absorption of more positive ions [49]. In the $M_3$ membrane with 0.03% w.t of glycidyl-pass, the yield has decreased to a small amount. The increase in porosity and the average size of the holes has caused the passage of Na+ ions and this has resulted in a decrease in yield. In the $M_4$ membrane with 0.3% w.t of glycidyl-pass, we have seen an increase in the yield. Increasing the amount of glycidyl-pass has caused the increase of functional groups in this membrane. Electrostatic repulsion between functional groups with negative charge and $SO4^{-2}$ ions, as well as more absorption of

$Na^+$ ions on the surface of the membrane and within the structure of the membrane due to the presence of glycidyl-pass with a porous structure, increases the yield [9,10,50-53].

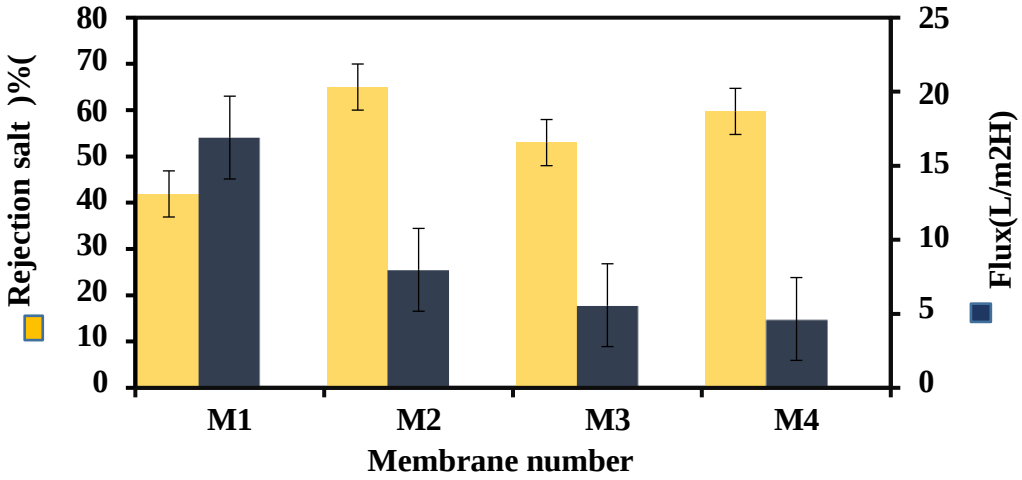


**Fig.10.** The flux and salt rejection results

## 3.6. Heavy metal removal experiment

The results of the removal of $CrSO_4$ metal shows in Fig.11. As evidenced by the results, the modified membranes exhibited an upward trajectory in efficiency. In the $M_2$ membrane, because of the presence of hydroxyl and carboxyl functional groups, the electrostatic repulsion between the functional groups and $SO4^{-2}$ ions has increased the yield. In the M3 membrane, due to the increase in flux and porosity, more ions have passed through the membrane, as a result, the yield has decreased slightly compared to $M_2$. In the M4 membrane, increasing the amount of glycidyl-pass, more $Cr^{2+}$ ions are trapped and absorbed due to the porous structure of glycidyl-pass, thus increasing the yield [46,51].

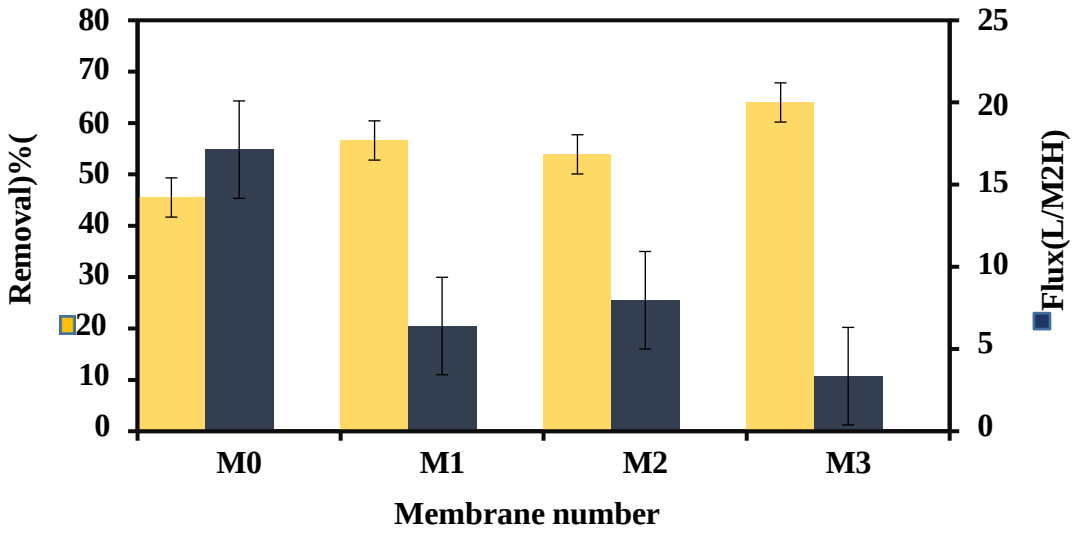


**Fig.11.** Heavy metal ions removal

### 3.7. Flux recovery ratio

The most crucial factor in reducing membrane clogging is to enhance the surface properties, particularly the hydrophilicity. The anti-fouling properties of the prepared membranes can be evaluated by measuring the reduction ratio of the passing flux [48]. Also, the result of the flux recovery ratio is shown in Fig.13. According to the result, the $M_2$ membrane has better antifouling properties than other membranes. The presence of hydrophilic groups on the surface of the membrane improves the anti-clogging properties of the membranes. Improving the structure and surface properties of the membrane can reduce membrane fouling [49,50]. In M3 and $M_4$ membranes, with the decrease in hydrophilicity and increase in surface roughness, due to the formation of AA-g-POSS on the membrane surface, the percentage of flux recovery has decreased [51,53].

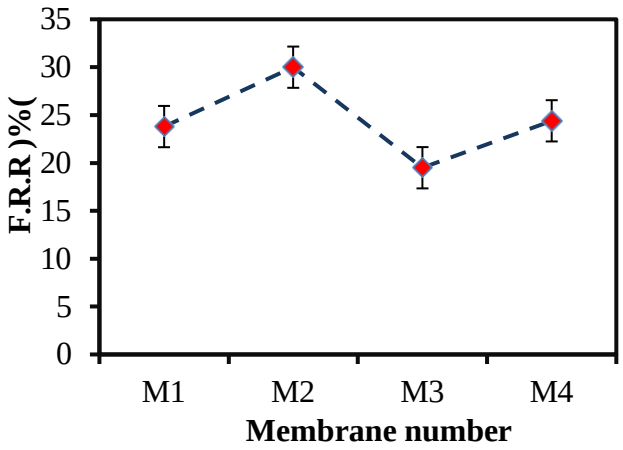


**Fig.12.** The flux recovery ratio (FRR%) of pristine membrane and modified membrane

### 3.8. Mechanical tensile strength experiment

The results of the tensile strength measurement are illustrated in Fig. 12. The obtained results indicate that the tensile strength of the modified membranes is higher than that of the pure polyethersulfone membrane. The tensile strength of the M2 membrane has increased as a result of the polymerization of acrylic acid on its surface and the formation of robust bonds. The formation of AA-g-POSS on the surface of the M3 membrane results in a stronger interaction than that observed in the pure polymer mixture, leading to an increase in tensile strength. However, in the M4 membrane, the accumulation and lumpiness of glycidyl-pass nanoparticles cause a loosening of the bond between the polymer chains, resulting in a decrease in tensile strength [39,51].

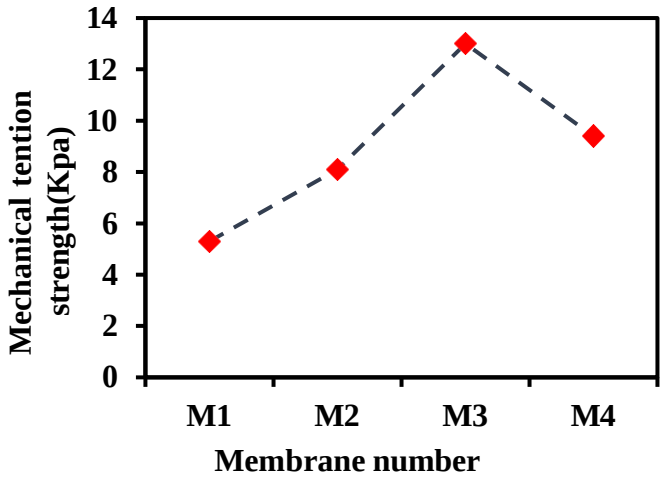


**Fig.12.** The tensile strength

## 4. Conclusion

In this research, nanofiltration membranes were fabricated via the phase inversion method. Subsequently, the membranes were subjected to modification through the incorporation of varying weight percentages of glycidyl-pass nanoparticles. The surface modification resulted in the formation of a dense layer on the surface of the membrane, which led to a reduction in the pure water flux in comparison to the neat membrane. The findings of the contact angle analysis indicate that the membrane exhibited an increasing hydrophilic property initially, followed by a decline in this property with an increase in the weight percentage of glycidyl-pass. An increase in the amount of glycidyl phosphate resulted in an expansion of the average pore size. However, the accumulation of nanoparticles within the membrane pores led to a reduction in porosity. The recovery rate of sodium sulfate and chromium sulfate for modified membranes is increased in comparison to the pure membrane. The anti-clogging property of the membrane initially improved and then decreased with the increase in the weight percentage of glycidyl-pass and the surface roughness. The amount of tensile strength increased with surface modification of the pure polyethersulfone membrane by nanoparticles.

## Conflicts of Interest

The author declares no conflict of interest.

## Author information

*Corresponding Author: Abdolreza Mogaddasi, Samaneh Bandeh Ali
E-mail address: a-moghadassi@araku.ac.ir, s.bandehali@abru.ac.ir

## References

[1] K. Nat, Membrane Separation Processes, Prentice Hall of India Private Limited, New Delhi-110001, G.C.E.T, 2008. https://doi.org/10.1007/978-1-4615-4269-8_1.

[2] T.A. Saleh, V.K Gupta, Synthesis and characterization of alumina nano-particles polyamide membrane with enhanced flux rejection performance, Sep. Purif. Technol, 89 (2012) 245-251. https://doi.org/10.1016/j.seppur.2012.01.039.

[3] V. Vatanpour, S.S. Madaeni, R. Moradian, S. Zinadini, B. Astinchap, Fabrication and characterization of novel antifouling nanofiltration membrane prepared from oxidized multiwalled carbon nanotube/polyethersulfone nanocomposite, J. Member. Sci. 375 (2011) 284–294. https://doi.org/10.1016/j.memsci.2011.03.055.

[4] Z. Huang, L. Lu, Z. Cai, Z.J. Ren, Individual and competitive removal of heavy metals using capacitive deionization, J. Hazard Mater. 302 (2016) 323–331. https://doi.org/10.1016/j.jhazmat.2015.09.064.

[5] S.M. Hosseini, S.S. Madaeni, A.R. Khodabakhshi, A. Zendehnam, preparation and surface modification of PVC/SBR heterogeneous cation exchange membrane with silver nanoparticles by plasma treatment, J. member. Sci. 365 (2010) 438–446. https://doi.org/10.1016/j.memsci.2010.09.043.

[6] A. Peterlin, Dependence of diffusive transport on morphology of crystalline polymers, J. Macromol. Sci. Phys, 11 (1975) 57-87. https://doi.org/10.1080/00222347508217855.

[7] C.-C. Yang, Y.J. Li, T.-H. Liou, Preparation of novel poly (vinyl alcohol)/SiO2 nanocomposite membranes by a sol–gel process and their application on alkaline DMFCs, Desalination, 276 (2011) 366-372. https://doi.org/10.1016/j.desal.2011.03.079.

[8] F. Zareei, S.M. Hosseini, A new type of polyethersulfone based composite nanofiltration membrane decorated by cobalt ferrite-copper oxide nanoparticles with enhanced performance and antifouling property, Separ. Purif. Technol. 226 (2019) 48–58. https://doi.org/10.1016/j.seppur.2019.05.077.

[9] S. Hosseini, F. Moradi, S. Koudzari Farahani, S. Bandehali, F. Parvizian, M. Ebrahimi, J. Shen, Carbon nanofibers/chitosan nanocomposite thin film for surface modification of poly (ether sulphone) nanofiltration membrane, Mater. Chem. Phys., (2021). https://doi.org/10.1016/j.matchemphys.2021.124720.

[10] V. Moghimifar, A. Raisi, A. Aroujalian, Surface modification of polyethersulfone ultrafiltration membranes by corona plasma-assisted coating TiO2 nanoparticl, J. Membr. Sci., 461 (2014) 69–80. https://doi.org/10.1016/j.memsci.2014.02.012.

[11] S. Bandehali, F. Parvizian, A.R. Moghadassi, S.M. Hosseini, J.N. Shen, Fabrication of thin film-PEI nanofiltration membrane with promoted separation performances: Cr, Pb and Cu ions removal from water, J. Polym. Res., 27 (2020) 94. https://doi.org/10.1007/s10965-020-02056-x.
[12] Y. Zhang, Y. Wan, Y. Shi, G. Pan, H. Yan, J. Xu, M. Guo, L. Qin, Y. Liu, Facile modification of thin-ilm composite nanofiltration membrane with silver nanoparticles for anti-biofouling, J. Polymer Res, 23 (2016) 105–114. 10.1007/s10965-016-0992-7.
[13] C. Williams, R. Waheman, Membrane fouling and alternative techniques for its alleviation, Member, Technol. 2000 (2000) 4–10. https://doi.org/10.1016/S0958-2118(00)80017-8.
[14] W.P. Zhu, J. Gao, S.P. Sun, S. Zhang, T.S. Chung, Poly (amidoamine) dendrimer (PAMAM) grafted on thin film composite (TFC) nanofiltration (NF) hollow fiber membranes for heavy metal removal, J. Member. Sci. 487 (2015) 117–126. https://doi.org/10.1016/j.memsci.2015.03.033.
[15] S.Y. Wu, J.X, C. Zheng, G.F. Xu, G.D. Zheng and J.P. Xu, J. Appl. Polym. Sci. 64 (1977) 1923-1926.
[16] A. Kulkarni, D. Mukherjee, W.N. Gill, Flux enhancement by hydrophilization of thin film composite reverse osmosis membranes, JMSR, 114 (1996) pp. 39-50. https://doi.org/10.1016/0376-7388(95)00271-5.
[17] S. Tul Muntha, A. Kausar, M. Siddiq, Advances in polymeric nanofiltration membrane: A review, POLYM-PLAST TECHNOL, 56 (2017) 841-856. https://doi.org/10.1080/03602559.2016.1233562.
[18] H. Hachisuka, K. dIkeda, Composite reverse osmosis membrane having a separation layer with polyvinyl alcohol coating and method of reverse osmotic treatment of water using the same, Google Patents, (2001).
[19] S.M. Hosseini, F. Karami, S.K. Farahani, S. Bandehali, J.N. Shen, E. Bagheripour, A. Seidypoor, Tailoring the separation performance and antifouling property of polyethersulfone based NF membrane by incorporating hydrophilic CuOnanoparticles, Kor. J. Chem. Eng. 37 (2020) 866–874. https://doi.org/10.1007/s11814-020-0497-2.
[20] C. Zhao, J. Xue, F. Ran, S. Sun, Modification of polyethersulfone membranes–a review of methods, Prog. Mater. Sci, 58 (2013) 76-150. https://doi.org/10.1016/j.pmatsci.2012.07.002.
[21] S. Bandehali, A. Moghadassi, F. Parvizian, S.M. Hosseini, A new type of [PEI-glycidyl POSS] nanofiltration membrane with enhanced separation and antifouling performance, Korean J. Chem. Eng, 36 (2019) 1657-1668. https://doi.org/10.1007/s11814-021-0831-3
[22] S. Bandehali, F. Parvizian, A. Moghadassi, S.M. Hosseini, Copper and lead ions removal from water by new PEI based NF membrane modified by functionalized POSS nanoparticles, J. Polym, (2019) 211. https://doi.org/10.1007/s10965-019-1865-7.
[23] V.Vatanpour, M. Esmaeili, M. Safarpour, A. mGhadimi, J. Adabi, Synergistic effect of carboxylated-MWCNTs on the performance of acrylic acid UV-grafted polyamide nanofiltration membranes, React. Funct. Polym, 134 (2019) 74-84. https://doi.org/10.1016/j.reactfunctpolym.2018.11.010.
[24] L. Li, Z. Yin, F. Li, T. Xiang, Y. Chen, C. Zhao, Preparation and characterization of poly (acrylonitrile-acrylic acid-N-vinyl pyrrolidinone) terpolymer blended polyethersulfone membranes, J. Membr. Sci, 349 (2010) 56-64. https://doi.org/10.1016/j.memsci.2009.11.018.
[25] S.-H. Chen, R.-M. Liou, C.-L Lai, M.-Y. Hung, M.-H. Tsai, S.-L. Huang, Embedded nano-iron polysulfone membrane for dehydration of the ethanol/water mixtures by pervaporation, Desalination, 234 (2008) 221-231. https://doi.org/10.1016/j.desal.2007.09.089.
[26] G.-J. Hwang, H. Ohya, T. Nagai, Ion exchange membrane based on block copolymers. Part III: preparation of cation exchange membrane, J. Membr. Sci, 156 (1999) 61-65.
[27] N. Ghaemi, S.S. Madaeni, P. Daraei, H. Rajabi, T. Shojaeimehr, F. Rahimpour, B. Shirvani, PES mixed matrix nanofiltration membrane embedded with polymer wrapped MWCNT: Fabrication and performance optimization in dye removal by RSM, J. Hazard. Mater, 298 (2015) 111-121. https://doi.org/10.1016/j.jhazmat.2015.05.018.
[28] E. Bagheripour, A. Moghadassi, S. Hosseini, B. Van der Bruggen, F. Parvizian, Novel composite graphene oxide/chitosan nanoplates incorporated into PES based nanofiltration membrane: chromium removal and antifouling enhancement, J.I.E.C, 62 (2018) 311-320. https://doi.org/10.1016/j.jiec.2018.01.009.
[29] Q. Zhang, L. Fan, Z. Yang, R. Zhang, Y.-n. Liu, M. He, Y. Su, Z. Jiang, Loose nanofiltration membrane for dye/salt separation through interfacial polymerization with in-situ generated $TiO_2$ nanoparticles, Appl. Surf. Sci, 410 (2017) 494-504. https://doi.org/10.1016/j.apsusc.2017.03.087.

[30] L.Y. Ng, A.W. Mohammad, C.P. Leo, N. Hilal, Polymeric membranes incorporated with metal/metal oxide nanoparticles: a comprehensive review, Desalination, 308 (2013) 15-33. https://doi.org/10.1016/j.desal.2010.11.033.
[31] P. Mobarakabad, A.R. Moghadassi, S.M. Hosseini. Fabrication and characterization of poly (phenylene ether-ether sulfone) based nanofiltration membranes modified by titanium dioxide nanoparticles for water desalination, Desalination 365 (2015) 227–233. https://doi.org/10.1016/j.desal.2015.03.002.
[32] A. Gholami, A. Moghadassi, S.M. Hosseini, S. Shabani, F. Gholami, Preparation and characterization of polyvinyl chloride based nanocomposite nanofiltration-membrane modified by iron oxide nanoparticles for lead removal from waterJ.I.E.C, 204 (2014) 1517-1522. https://doi.org/10.1016/j.jiec.2013.07.041.
[33] M. Safarpour, V. Vatanpour, A. Khataee, Preparation and characterization of graphene oxide/TiO2 blended PES nanofiltration membrane with improved antifouling and separation performance, Desalination, 393 (2016) 65-78. https://doi.org/10.1016/j.desal.2015.07.003.
[34] H. Abdul Mannan, H. Mukhtar, M. Shima Shaharun, M. Roslee Othman, T. Murugesan, Polysulfone/poly (ether sulfone) blended membranes for $CO_2$ separation, J. Appl. Polym. Sci, 133 (2016).
[35] A. Qin, X. Li, X. Zhao, D. Liu, C. He, Engineering a highly hydrophilic PVDF membrane via binding TiO2 nanoparticles and a PVA layer onto a membrane surface, ACS Appl. Mater. Interfaces, 7 (2015) 8427-8436. https://doi.org/10.1021/acsami.5b00978.
[36] N. Ghaemi, S.S. Madaeni, A. Alizadeh, H. Rajabi, P. Daraei, Preparation, characterization and performance of polyethersulfone/organically modified montmorillonite nanocomposite membranes in removal of pesticides, J. Membr. Sci, 382 (2011) 135-147. https://doi.org/10.1016/j.memsci.2011.08.004.
[37] M.R.S. Kebria, M. Jahanshahi, A. Rahimpour, $SiO_2$ modified polyethyleneimine-based nanofiltration membranes for dye removal from aqueous and organic solutions, Desalination, 367 (2015) 255-264. https://doi.org/10.1016/j.desal.2015.04.017.
[38] E. Bagheripour, A. Moghadassi, S. Hosseini, M. Ray, F. Parvizian, B. Gt Bruggen, Highly hydrophilic and antifouling nanofiltration membrane incorporated with water-dispersible composite activated carbon/chitosan nanoparticles, Chem. Eng. Res. Des., 132 (2018) 812-821. https://doi.org/10.1016/j.cherd.2018.02.027
[39] M.R. Mehrnia, Y.M. Mojtahedi, M. Homayoonfal, What is the concentration threshold of nanoparticles within the membrane structure? A case study of $Al_2O_3$/PSf nanocomposite membrane, Desalination, 372 (2015) 75-88. https://doi.org/10.1016/j.desal.2015.06.022.
[40] N. Rakhshan, M. Pakizeh, The effect of functionalized $SiO_2$ nanoparticles on the morphology and triazines separation properties of cellulose acetate membranes, J.I.E.C, 34 (2016) 51-60.
[41] L. Jin, W. Shi, S. Yu, X. Yi, N. Sun, C. Ma, Y. Liu, Preparation and characterization of a novel PA-$SiO_2$ nanofiltration membrane for raw water treatment, Desalination, 298 (2012) 34-41. https://doi.org/10.1016/j.desal.2012.04.024.
[42] M. Khorram, F. Nabizadeh Chianeh, M. Shamsodin, Preparation and characterization of a novel polyethersulfone nanofiltration membrane modified with $Bi_2O_3$ nanoparticles for enhanced separation performance and antifouling properties, J.I.E.C, (2022). https://doi.org/10.1016/j.jiec.2022.07.036.
[43] P. DaraeiMadaeni, S.S., Salehi, E., Ghaemi, N., Ghari, H.S., Khadivi, M.A., Rostami, E., Novel thin film composite membrane fabricated by mixed matrix nanoclay/chitosan on PVDF microfiltration support: Preparation, characterization and performance in dye removal, J. Membr. Sci, 436 (2013) 97-108. https://doi.org/10.1016/j.memsci.2013.02.031.
[44] S. Hosseini, M. Nemati, F. Jeddi, E. Salehi, A. Khodabakhshi, S. Madaeni, Fabrication of mixed matrix heterogeneous cation exchange membrane modified by titanium dioxide nanoparticles: Mono/bivalent ionic transport property in desalination, Desalination, 359 (2015) 167-175. https://doi.org/10.1016/j.desal.2014.12.043.
[45] A. Salimi, A. Yousefi, Analysis method: FTIR studies of β-phase crystal formation in stretched PVDF films, Polym. Test., 22 (2003) 699-704. https://doi.org/10.1016/S0142-9418(03)00003-5.
[46] Y. He, Y.P. Tang, T.S. Chung, Concurrent removal of selenium and arsenic from water using polyhedral oligomeric silsesquioxane (POSS)–polyamide thin-film nanocomposite nanofiltration membranes, Ind. Eng. Chem. Res, 55 (2016) 12929-12938. https://doi.org/10.1021/acs.iecr.6b04272.

[47] Y. Zhang, S. Zhang, T.-S. Chung, Nanometric graphene oxide framework membranes with enhanced heavy metal removal via nanofiltration, Environ. Sci. Technol, 49 (2015) 10235-10242. https://doi.org/10.1021/acs.est.5b02086.
[48] J.H. Moon, A.R. Katha, S. Pandian, S.M. Kolake, S. Han, Polyamide–POSS hybrid membranes for seawater desalination: Effect of POSS inclusion on membrane properties, J. Membr. Sci., 462 (2014) 89-95. https://doi.org/10.1016/j.memsci.2014.03.004.
[49] E.G. Vieira, I.V. Soares, G. Pires, R.A. Ramos, D.R. do Carmo, N.L. Dias Filho, Study on determination and removal of metallic ions from aqueous and alcoholic solutions using a new POSS adsorbent, J. Chem. Eng, 264 (2015) 77-88. https://doi.org/10.1016/j.cej.2014.11.050.
[50] S. Koudzari Farahani, S.M. Hosseini, A highly promoted nanofiltration membrane by incorporating of aminated Zr-based MOF for efficient salts and dyes removal with excellent antifouling properties, Chem. Eng. Res. Des, (2022). https://doi.org/10.1016/j.cherd.2022.10.027.
[51] M. Amirilargani, M. Sadrzadeh, E. Sudhölter, L. De Smet, Surface modification methods of organic solvent nanofiltration membranes, J. Chem. Eng., 289 (2016) 562-582. https://doi.org/10.1016/j.cej.2015.12.062.
[52] S. Madaeni, S. Zinadini, V. Vatanpour, Preparation of superhydrophobic nanofiltration membrane by embedding multiwalled carbon nanotube and polydimethylsiloxane in pores of microfiltration membrane, Sep. Purif. Technol., 111 (2013) 98-107. https://doi.org/10.1016/j.seppur.2013.03.033.
[53] Y. Mansourpanah, A. Rahimpour, M. Tabatabaei, L. Bennett, Self-antifouling properties of magnetic $Fe_2O_3/SiO_2$-modified poly (piperazine amide) active layer for desalting of water: Characterization and performance, Desalination, 419 (2017) 79-87. https://doi.org/10.1016/j.desal.2017.06.006.